



www.serid.ait.ac.th/eric

## Improving the Stability of a Distribution System Embedded with Wind Turbine Induction Generators Using STATCOM

S. Panda<sup>\*1</sup> and N.P. Padhy<sup>+</sup>

**Abstract** – This paper deals with stability improvement of a distribution system embedded with wind turbine induction generators (WTIGs), by using a Static Synchronous Compensator (STATCOM). The dynamic behavior of a distribution system, during an external three-phase fault and under various types of wind speed changes, is investigated. The study is carried out by three-phase, non-linear, dynamic simulation of distribution system component models. Simulation results are presented for two control strategies of STATCOM (namely the voltage and the var control mode), and four types of wind speed changes. Simulation results show that the var control mode is more effective in maintaining the stability and the WTIGs remain connected to the distribution system, compared to the voltage controlled mode. Further, it is also noticed that, the voltage control mode of operation of the STATCOM, gives better voltage stability performance in the example distribution system compared to the var control mode of operation.

**Keywords** – Distribution system, reactive power compensation, speed stability, STATCOM, voltage stability, wind turbine induction generator.

### 1. INTRODUCTION

The rapid development of Distributed Generation (DG) technology is gradually reshaping the conventional power systems in a number of countries. Wind power is among the most actively developing DG technology. Grid-connected wind capacity is undergoing the fastest rate of growth compared to any form of electricity generation, achieving global annual growth rates in the order of 20 - 30% [1]. It is clear that the benefit from connecting wind generations is significant subject to a conversion of passive to active distribution network. This is because the technical as well as commercial planning frameworks of the present scenarios have not been designed keeping DG's in mind. If we place distributed generators in randomly or one by one basis that may lead to excess investment over a long period of time as well as it may sterilize the network. Distribution network sterilization results when capacity is allocated to the buses whose voltage and short circuit levels are most sensitive to power injections and hence no more generators are allowed to connect at those buses. The wind embedded generations are responsible for voltage rise but if connected at highly loaded node, may help the network. During off-peak period the absorption of reactive power by the wind generator may control the voltage rise effect. Presence of wind generator became a problem for protection, stability, reverse power flow and investment issues but provides cheap and green power [2].

The presence of wind power generation is likely to influence the operation of the existing power system networks, especially the power system stability. After the

clearance of a short-circuit fault in the external network, the grid connected wind turbine should restore its normal operation without disconnection caused by inrush current and dipped voltage. The protective disconnection of a large amount of wind power may cause an important loss of generation that may threaten the power system stability [3], [4]. Further, dynamic changes of wind speed make amount of power injected to a network highly variable. Depending on intensity and rate of changes, difficulties with frequency, voltage regulation and stability, could make a direct impact to quality level of delivered electrical energy [5]. In this context, from stability viewpoint, connection of wind turbine generator with dispersed generation of electricity, calls for a detailed technical analysis.

Majority of the wind power based DG technologies employ Induction Generators (IG) instead of synchronous generators, for the technical advantages of IG like: reduced size, increased robustness, lower cost and increased electromechanical damping. However, IGs draw very large reactive currents during fault occurrence [6]. Wind Turbine Induction Generator (WTIG) can be viewed as a consumer of reactive power. Its reactive power consumption depends on active power production. Conventionally, shunt capacitor banks are connected at the generator terminals to compensate its reactive power consumption.

To minimize reactive power exchange between wind power plant and distribution network, dynamic compensation of reactive power can be employed [5]-[7]. Further, the normal operation restoration after the clearance of an external system fault can be improved with dynamic reactive compensation. Without the dynamic compensation, it is possible that at some locations only a small number of wind turbines could be connected due to weak voltage conditions. This would not only leave assessed wind potential unused, but it could also prohibit installation of larger number of wind turbines thus jeopardizing the economics of the whole project.

<sup>\*</sup>National Institute of Science and Technology (NIST), Brahmapur, Orissa, Pin-761008, India.

<sup>+</sup>Indian Institute of Technology Roorkee, Uttarakhand, Pin-247667, India.

<sup>1</sup> Corresponding author; Tel: + 91 943 825 1162.  
E-mail: [panda\\_sidhartha@rediffmail.com](mailto:panda_sidhartha@rediffmail.com)

Recent development of power electronics introduces the use of Flexible AC Transmission System (FACTS) controllers in power systems [8]. Shunt FACTS controllers play an important role in controlling the reactive power flow in the power network, which in turn affects the system voltage fluctuation and transient stability. The STATCOM is one of the important FACTS devices and can be used for dynamic reactive power compensation of power systems to provide voltage support and stability improvement [9]. Application of STATCOM to improve stability improvement has been reported in the literature [10]-[12]. Most of the studies report improvement of one type of stability, either transient stability or voltage stability and in almost all cases single phase model have been used. In the present study, the effect of a STATCOM in improving both the transient stability and voltage stability of the distributed network with WTIGs is studied. The study is based on the 3-phase non-linear dynamic simulation, utilizing the SimPowerSystem blockset for use with MATLAB/SIMULINK [13]. In order to overcome negative dynamic impacts caused by WTIGs, a STATCOM is used at the point of WTIGs and distribution network connection. Simulation results are presented to show the improved stability performance of a distributed network embedded with WTIGs under severe disturbances with the use of a STATCOM. Further, the effects of different types of wind speeds and different control mode of operation of STATCOM on the performance of a distribution system are presented and analyzed. Further, the effects of different types of wind speed changes and different control mode of operation of STATCOM on the performance of a distribution system are presented.

**2. DISTRIBUTION SYSTEM COMPONENTS MODELS**

Distribution systems are in most of the cases unbalanced due to the asymmetrical line spacing and imbalance of customer load. Single phase models may not give accurate results when studies on the operation of distributed systems are carried out. Therefore in this work all network components are represented by the 3-phase models [13].

The block diagram of wind turbine induction generator (WTIG) is shown in Figure 1. The stator winding is connected directly to the 60 HZ grid and the rotor is driven by a variable-pitch wind turbine. The power captured by the wind turbine is converted into electrical power by the induction generator and is transmitted to the grid by the stator winding. For high wind speeds, the pitch angle is controlled to limit the generator output power to its nominal value. To generate power the induction generator speed must be slightly above the synchronous speed. The pitch angle controller regulates the wind turbine blade pitch angle  $\beta$ , according to the wind speed variations. Hence, the power output of WTIG depends on the characteristics of the pitch controller in addition to the turbine and generator characteristics. This control guarantees that, irrespective of the voltage, the power output of the WTIG for any wind speed will be equal to the designed value for that speed. The designed power output of the WTIG with wind speed is provided by the manufacturer in the form of a

power curve. For a given wind speed, power output can be obtained from the power curve of the WTIG.

The pitch angle control system is shown Figure 2. To limit the electric output power to the nominal mechanical power, a PI controller is used to control the blade pitch angle. When the measured electric output power is under its nominal value, the pitch angle is kept steady at zero degree. The PI controller increases the pitch angle when the measured power increases above its nominal value to bring back it to its nominal value. The pitch angle is controlled in order to limit the generator output power at its nominal value for winds exceeding the nominal speed. Each wind turbine has a protection system monitoring voltage, current and machine speed.

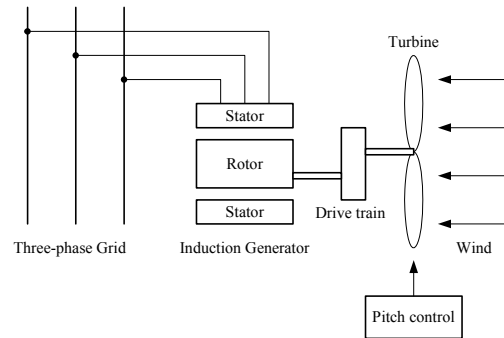


**Fig. 1. Block diagram of WTIG.**

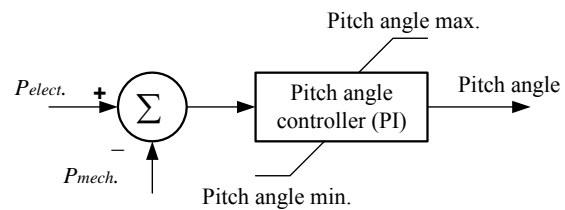


**Fig. 2. Pitch angle control system.**

**Wind Turbine**

The wind turbine model employed in the present study is based on the steady-state power characteristics of the turbine. The stiffness of the drive train is assumed infinite and the friction factor and the inertia of the turbine are combined with those of the generator coupled to the turbine. The wind turbine mechanical power output is a function of rotor speed as well as the wind speed and is expressed as:

$$P_m = C_p(\lambda, \beta) \frac{\rho A}{2} V_{wind}^3 \tag{1}$$

Equation 1 can be normalized in the per unit (pu) system as:

$$P_{m\_pu} = k_p C_{p\_pu} V_{wind\_pu}^3 \tag{2}$$

A generic equation is used to model  $C_p(\lambda, \beta)$ . This equation, based on the modeling turbine characteristics is:

$$C_p(\lambda, \beta) = c_1 \left( \frac{c_2}{\lambda_i} - c_3 \beta - c_4 \right) e^{-\frac{c_5}{\lambda_i}} + c_6 \lambda \tag{3}$$

where,  $P_m$  = Mechanical output power of the turbine (W)

$C_p$  = Performance coefficient of the turbine

$\rho$  = Air density (kg/m<sup>3</sup>)

$A$  = Turbine swept area (m<sup>2</sup>)

$V_{wind}$  = Wind speed (m/s)

$\lambda$  = Tip speed ratio of the rotor blade tip speed to wind speed

$\beta$  = Blade pitch angle (deg)

$P_{m\_pu}$  = Power in pu of nominal power for particular values of  $\rho$  and  $A$

$C_{p\_pu}$  = Performance coefficient in pu of the maximum value of  $C_p$

$k_p$  = Power gain

$$\frac{1}{\lambda_i} = \frac{1}{\lambda + 0.08\beta} - \frac{0.035}{\beta^3 + 1}$$

The relevant parameters are given in Appendix.

### Induction Machine

In the present study, the electrical part of the machine is represented by a second-order state-space model and the mechanical part by a second-order system. All electrical variables and parameters are referred to the stator. All stator and rotor quantities are in the arbitrary two-axis reference frame ( $d$ - $q$  frame). The  $d$ -axis and  $q$ -axis block diagram of the electrical system is shown in Figures 3 and 4, respectively.

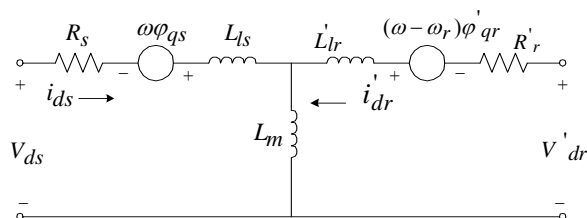


**Fig. 3. Induction machine  $d$ -axis equivalent circuit.**

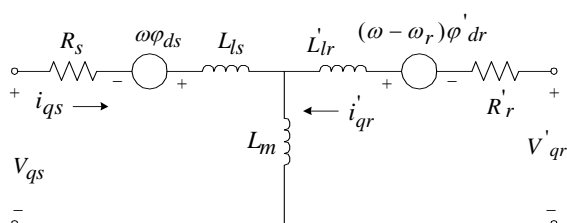


**Fig. 4. Induction machine  $q$ -axis equivalent circuit.**

The electrical equations are given by:

$$v_{qs} = R_s i_{qs} + \frac{d}{dt} \phi_{qs} + \omega \phi_{ds} \quad (4)$$

$$v_{ds} = R_s i_{ds} + \frac{d}{dt} \phi_{ds} - \omega \phi_{qs} \quad (5)$$

$$v'_{qr} = R'_r i_{qr} + \frac{d}{dt} \phi'_{qr} + (\omega - \omega_r) \phi'_{dr} \quad (6)$$

$$v'_{dr} = R'_r i_{dr} + \frac{d}{dt} \phi'_{dr} - (\omega - \omega_r) \phi'_{qr} \quad (7)$$

$$T_e = 1.5p(\phi_{ds} i_{qs} - \phi_{qs} i_{ds}) \quad (8)$$

where,  $\phi_{qs} = L_s i_{qs} + L_m i'_{qr}$ ;  $\phi_{ds} = L_s i_{ds} + L_m i'_{dr}$

$$\phi'_{qr} = L'_r i'_{qr} + L_m i_{qs}; \quad \phi'_{dr} = L'_r i'_{dr} + L_m i_{ds}$$

with  $L_s = L_{ls} + L_m$  and  $L'_r = L'_{lr} + L_m$

The mechanical equations are given by:

$$\frac{d}{dt} \omega_m = \frac{1}{2H} (T_e - F \omega_m - T_m) \quad (9)$$

$$\frac{d}{dt} \theta_m = \omega_m \quad (10)$$

where,  $R_s, L_{ls}$  = Stator resistance and leakage inductance

$R'_r, L'_{lr}$  = Rotor resistance and leakage inductance

$L_m$  = Magnetizing inductance

$L_s, L'_r$  = Total stator and rotor inductances

$V_{qs}, i_{qs}$  =  $q$ -axis stator voltage and current

$V'_{qr}, i'_{qr}$  =  $q$ -axis rotor voltage and current

$V_{ds}, i_{ds}$  =  $d$ -axis stator voltage and current

$V'_{dr}, i'_{dr}$  =  $d$ -axis rotor voltage and current

$\phi_{qs}, \phi_{ds}$  = Stator  $q$ -axis and  $d$ -axis fluxes

$\phi'_{qr}, \phi'_{dr}$  = Rotor  $q$ -axis and  $d$ -axis fluxes

$\omega_m$  = Angular velocity of the rotor

$\theta_m$  = Rotor angular position

$P$  = Number of pole pairs

$\omega_r$  = Electrical angular velocity

$\theta_r$  = Electrical rotor angular position

$T_e$  = Electromagnetic torque

$J$  = Combined rotor and load inertia coefficient

$H$  = Combined rotor and load inertia constant

$F$  = Combined rotor and load viscous friction coefficient

### Protection System

Commercial wind turbines incorporate sophisticated system for protection of electrical and mechanical components. These turbine-based protection system respond to local conditions, detecting grid or mechanical abnormalities that indicate system trouble or potentially damaging conditions for the turbine. The protection system should respond almost instantaneously to mechanical speed, vibration, voltages, or currents outside of defined tolerances. In addition, conventional multi-function relays for electric machine protection are generally provided to detect a wide variety of grid disturbances and abnormal conditions within the machine. In the present study the WTIG protection system consists of the following:

- Instantaneous / positive-sequence AC Over current.
- AC current imbalance.
- AC Over voltage / Under voltage (positive-sequence).
- AC Voltage unbalance (Negative-sequence / Zero-sequence).
- DC Over voltage.

### 3. STATIC SYNCHRONOUS COMPENSATOR

All The STATCOM is based on a solid state synchronous voltage source, which generates a balanced set of three sinusoidal voltages at the fundamental frequency, with rapidly controllable amplitude and phase angle. The functional block diagram model of the STATCOM is shown in Figure 5.

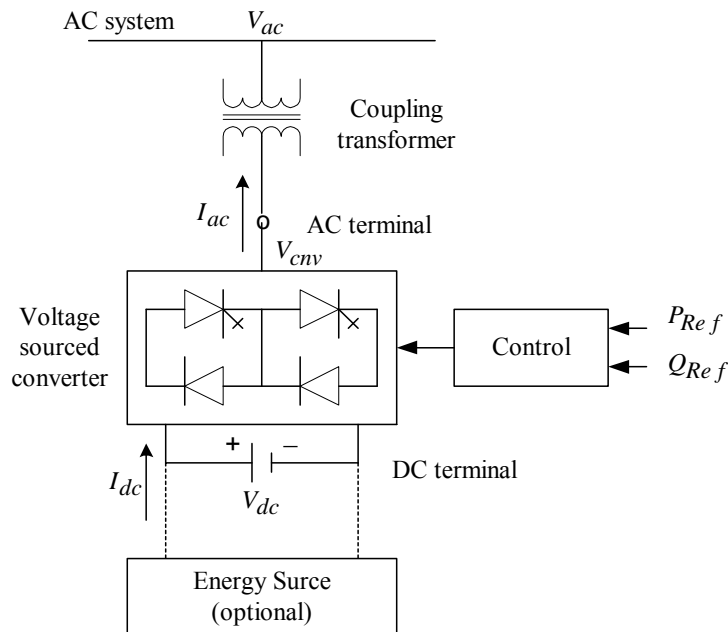


Fig. 5. Functional block diagram model of STATCOM.

The basic electronic block of a STATCOM is the Voltage Sourced Converter (VSC), which in general converts an input dc voltage into a three-phase output voltage at fundamental frequency, with rapidly controllable amplitude and phase angle. In addition to this, the controller has a coupling transformer and a dc capacitor. References  $Q_{Ref}$  and  $P_{Ref}$  define the magnitude and phase angle of the converter voltage  $V_{cnv}$  necessary to exchange the desired reactive and active power between the solid state voltage sourced converter and the ac system. If the device is operated strictly for reactive power exchange,  $P_{Ref}$  is set to zero and the external energy source is not required. The converter voltage  $V_{cnv}$  is in phase with the ac terminal voltage  $V_{ac}$  and there is practically no real power flow from or to VSC. The STATCOM supplies reactive power to the ac system if  $V_{cnv}$  is greater than  $V_{ac}$  and consumes reactive power if  $V_{cnv}$  is lower than  $V_{ac}$ . The device can be designed to maintain the magnitude of the bus voltage constant by controlling the magnitude and/or phase shift of the VSC output voltage.

Two types of technologies can be used for the VSC:

- VSC using GTO-based square-wave inverters and special interconnection transformers. Typically four three-level inverters are used to build a 48-step voltage waveform. Special interconnection transformers are used to neutralize harmonics contained in the square waves generated by individual inverters. In this type of VSC, the fundamental component of voltage  $V_{cnv}$  is

proportional to the voltage  $V_{DC}$ . Therefore  $V_{DC}$  has to be varied for controlling the injected voltage.

- VSC using IGBT-based pulse-width-modulation (PWM) inverters. This type of inverter uses PWM technique to synthesize a sinusoidal waveform from a DC voltage with a typical chopping frequency of a few kilohertz. Harmonics are cancelled by connecting filters at the AC side of the VSC. This type of VSC uses a fixed DC voltage  $V_{DC}$ . Voltage  $V_{cnv}$  is varied by changing the modulation index of the PWM modulator.

VSC using IGBT-based Pulse Width Modulation (PWM) inverters is used in the present study. However, as details of the inverter and harmonics are not represented in power system stability studies, the same model can be used to represent a GTO-based model.

Figure 6 shows a single-line diagram of the STATCOM and a simplified block diagram of its control system. The control system consists of [13]:

- A phase-locked loop (PLL) to synchronize on the positive-sequence component of the 3-phase primary voltage  $V_1$ . The direct-axis and quadrature-axis components of the AC 3-phase voltage and currents (labeled as  $V_d$ ,  $V_q$  and  $I_d$ ,  $I_q$  on the diagram) are computed using the output of the PLL.
- The measurement systems measuring the  $d$ -axis and  $q$ -axis components of AC positive-sequence voltage and currents to be controlled as well as the

DC voltage  $V_{DC}$ .

- The regulation loops, namely the AC voltage regulator and a DC voltage regulator. The output of the AC voltage regulator and DC voltage regulator are the reference current  $I_{qref}$  and  $I_{dref}$ , for the

current regulator.

- An inner current regulation loop consisting of a current regulator, which controls the magnitude and phase of the voltage generated by the PWM converter.

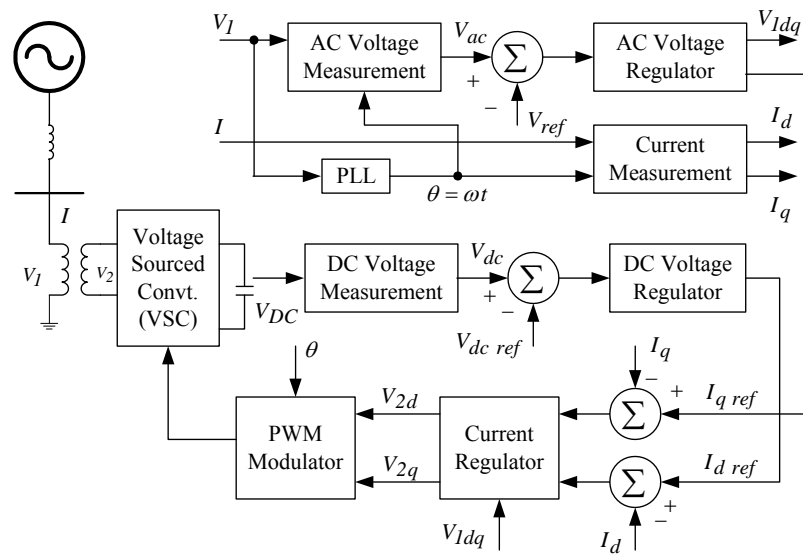


Fig. 6. Single-line diagram of a STATCOM and its control system.

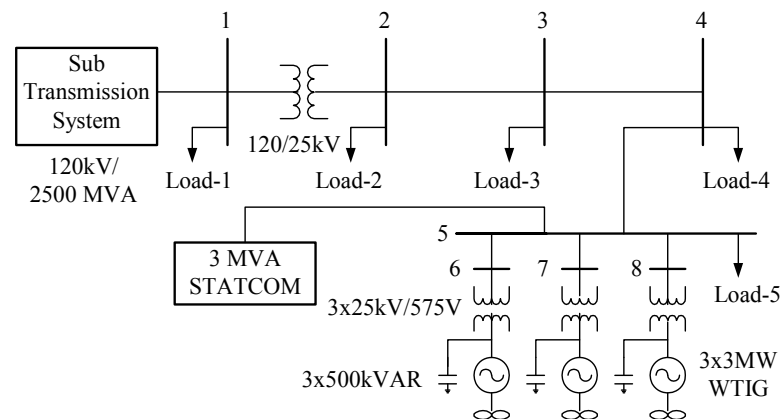


Fig. 7. Single-line diagram of the distribution system embedded with WTIGs and a STATCOM.

4. SYSTEM UNDER STUDY

The one-line diagram of the test system employed in this study is shown in Figure 7. The network consists of a 120 kV, 60 Hz, sub-transmission system with short circuit level of 2500 MVA, which feeds a 25 kV distribution system through 120/25 kV step down transformers. A 9 MW wind farm (consisting of six 1.5-MW wind turbines), connected to the 25 kV distribution system, exports power to the 120 kV grid. Part of the reactive power consumed by the WTIGs is locally supplied by fixed capacitors of 500 kVAR each, installed at the terminals of the machines. Dynamic reactive power compensation is provided by a 3 MVA STATCOM located at the point of WTIGs connection to the distribution network (bus 5). The relevant parameters are given in Appendix.

Wind turbines used in the present study use squirrel-cage induction generators. The stator winding is connected directly to the 60 Hz grid and the rotor is driven by a variable-pitch wind turbine. In order to limit the

generator output power at its nominal value, the pitch angle is controlled for winds exceeding the nominal speed of 9 m/s. Speed varies approximately between 1 pu at no load and 1.005 pu at full load. Each wind turbine has a protection system monitoring voltage, current and machine speed.

After the clearance of a short-circuit fault in the external network, the grid connected WTIGs should restore its normal operation without disconnection of WTIGs, caused by the protection system. The disconnection of a large amount of wind power may threaten the power system transient stability. Therefore, the transient stability issues are influenced by the amount of active power injected by WTIGs to the distribution network. Alternatively, as long as the WTIGs inject active power to the distribution network, transient stability is maintained [14].

**5. SIMULATION RESULTS**

The dynamic behavior of the WTIGs during an external 3-phase fault and different types of wind speed changes are analyzed and presented in this section. The active power generated by the WTIGs depends upon the wind speed. The types of wind speeds considered in the present study are: constant wind speed, linear change of wind speed, gust change of wind speed and random change of wind speed as shown in Figure 8. Further, two control mode of operation of STATCOM are considered namely; the

voltage control mode and the var control mode. The reference voltage and the reference reactive power are set to 1 pu for both control modes of operation.

Three cases are considered for all the types of wind speeds:

- Case-1: System without STATCOM.
- Case-2: System with STATCOM, operating in the voltage control mode.
- Case-3: System with STATCOM, operating in the var/power factor control mode.

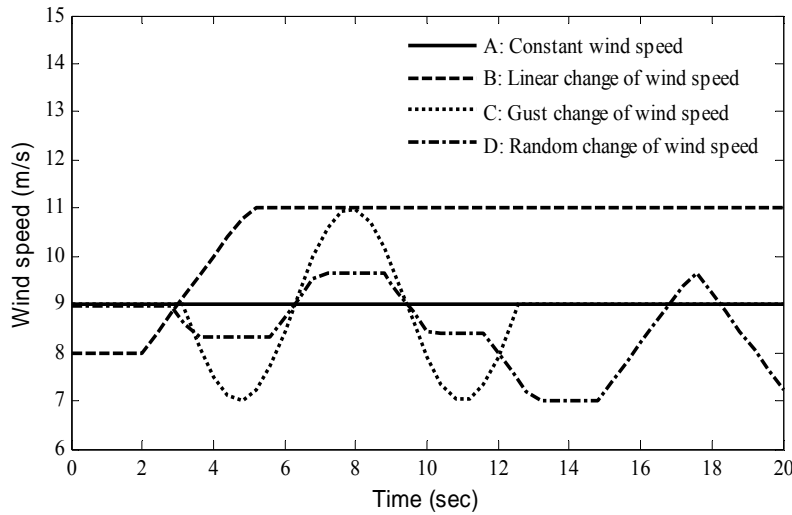


**Fig. 8. Types of wind speeds.**

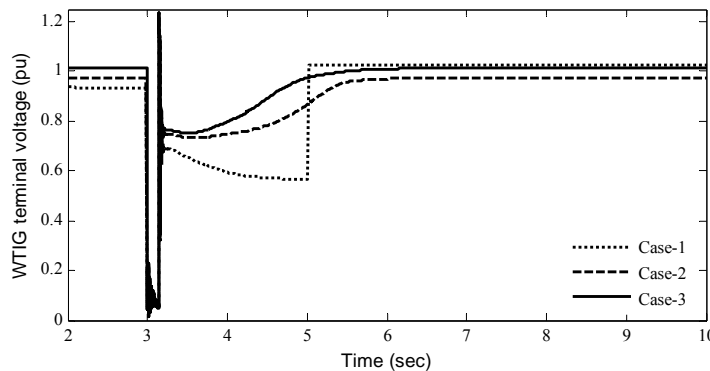


**Fig. 9. WTIG terminal voltage response for 9-cycle, 3-phase fault at bus 5 with constant wind speed angle.**

**Table 1. Critical clearing time for different types of faults.**

Type of fault/Fault bus	3-Ph	L-L-G	L-L	L-G
Bus-1	0.1383	0.2358	0.2815	0.6648
Bus-2	0.1362	0.2761	0.2761	1.9848
Bus-3	0.1281	0.2574	0.2574	1.9842
Bus-4	0.1184	0.2359	0.2358	1.9844
Bus-5	0.1128	0.2237	0.2236	1.9841

**Constant Wind Speed**

A constant wind speed of 9 m/s is applied to the wind turbine. In order to obtain the most severe situation for the example distribution system shown in Figure 7 many repeated simulations are conducted for different types of fault at different buses. The types of fault simulated are; three-phase fault, double line-to-ground fault, line-to-line fault and single line-to-ground fault. The critical clearing time (CCT) i.e. the maximum time duration for which the disturbance may act without the WTIGs losing its

capability to inject real power to the distribution network for all cases are summarized in Table 1. It can be seen from Table 1 that the most severe condition occurs when a 3-phase fault is applied at bus-5. In the present study, the most severe situation is considered for analysis.

A 3-phase fault is applied at the bus 5, at  $t = 3$  s and cleared after 9-cycles. The original system is restored upon the fault clearance. Figure 9 shows the response of WTIG terminal voltage (voltage at bus 6, 7 and 8) for the above contingency, for all the cases. It can be seen from

Figure 9 that, as the fault is applied near to the WTIGs (bus-5), the WTIG terminal voltage drops drastically on the occurrence of the fault. The low voltage condition starts at  $t=3$  s, at which the fault is applied and lasts for 9-cycles i.e. the duration of the fault. For case of system without STATCOM (shown in Figure 9, with legend Case-1), the WTIG terminal voltage becomes 0.68 pu immediately after the fault clearance. The AC Under voltage limit set by the protection system being equal to 0.75 pu, this low voltage condition results in tripping of WTIGs at  $t=5$  s. The tripping is initiated by the AC Under voltage protection. For the system with STATCOM (shown in Figure 9, with legends Case-2 and 3), because of reactive power support, the WTIG terminal voltage is above 0.75 pu immediately after the fault clearance. This value is within the limit set by the protection system. So the stability of the system is maintained and finally the WTIG terminal voltage recovers close to 1 pu for both the cases. Further, it can be seen from Figure 9 that, for the case of STATCOM operating in var control mode (Case-3), the terminal voltage is slightly more compared to the voltage control mode (Case-2). This is due to the fact that,

when the STATCOM is operating in voltage control mode (Case-2), the controller tries to maintain the terminal voltage constant at the preset reference value and the STATCOM supplies that much reactive power as is required to maintain the terminal voltage constant. But, when the STATCOM is operating in var control mode (Case-3), the controller tries to supply the preset reference reactive power.

The response of the active power injected into the distribution network ( $P_{INJ}$ ) is shown in Figure 10. In the pre-fault period, the value of  $P_{INJ}$  is equal to 8.71 MW. On the occurrence of the fault at  $t=3$  s,  $P_{INJ}$  reduces drastically for all the cases. For the case of system without STATCOM (Case-1), because of the tripping of the WTIGs,  $P_{INJ}$  become zero after the fault clearance. But, for the cases of system with STATCOM, operating in voltage control mode and var control mode (Case- 2 and 3), because of the reactive power support, the stability of the system is maintained. Hence, the WTIGs continue to inject real power to the distribution network after the fault clearance.

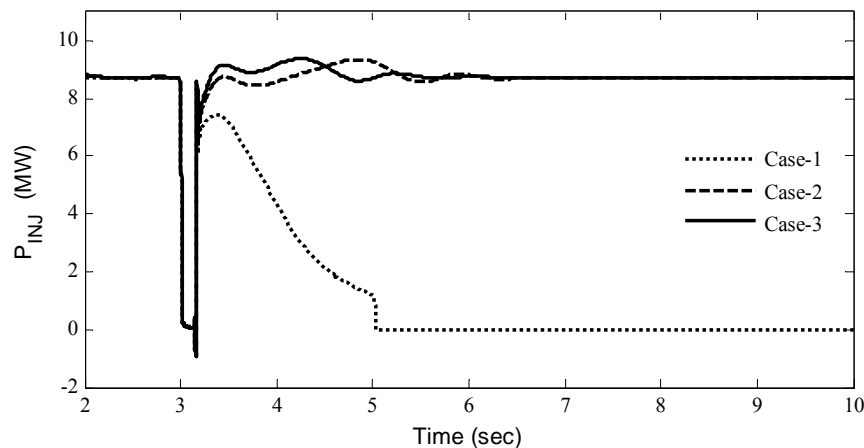


Fig. 10. Response of active power injected to the distribution network for 9-cycle, 3-phase fault at bus 5 with constant wind speed.

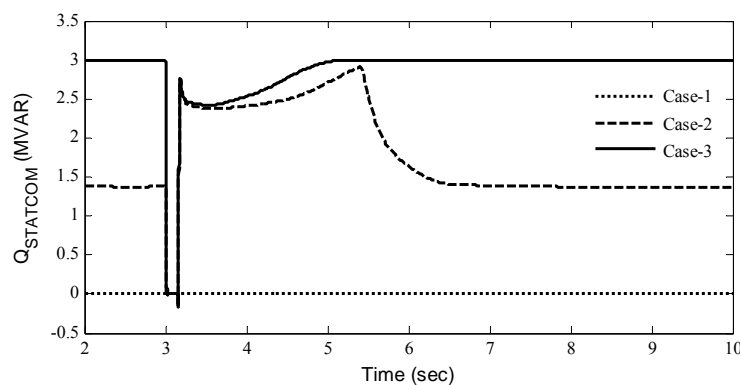


Fig. 11. Response of reactive power supplied by the STATCOM to the distribution network for 9-cycle, 3-phase fault at bus 5 with constant wind speed.

Figure 11 shows the variation of the reactive power supplied by the STATCOM ( $Q_{STATCOM}$ ) for the above contingency, for all the cases. When the STATCOM is inactive (Case-1),  $Q_{STATCOM}$  is obviously zero. It can also be seen from Figure 11 that, for the case of STATCOM operating in voltage control mode (Case-2), the controller tries to maintain the terminal voltage constant at the preset reference value and consequently the STATCOM supplies

that much reactive power as is required to maintain the terminal voltage constant. In case of STATCOM operating in var control mode (Case-3), as the reference reactive power is set to 1 pu, the controller tries to supply the rated reactive power. Hence  $Q_{STATCOM}$  for Case-3 is more than that of Case-2.

The response of WTIG speed for the above contingency is shown in Figure 12. The speed of the

WTIGs increases at the occurrence of the fault at  $t=3$  s, for all the cases. For the case of system without STATCOM (Case-1), as explained earlier, the system loses stability and the speed of the WTIGs continues to increase. For the system with STATCOM, operating in voltage control mode and var control mode (Case-2 and Case-3 respectively), stability of the system is maintained after the fault clearance. Further, it can be seen from Figure 12 that the WTIG speed for Case-2 is slightly more than that for Case-3. This is due to the fact that,  $Q_{STATCOM}$  is more in Case-3, compared to the Case-2. In the Case-2, the WTIGs draw the additional reactive power (i.e. the difference between the reactive power requirement of the WTIGs and  $Q_{STATCOM}$ ), from the distribution network. In order to draw more reactive power from the distribution network, the WTIGs are slightly overloaded in Case-2 compared to the Case-3. As a result, the WTIG speed is slightly more in Case-2 than in Case-3. From this, it can be concluded that, if the fault clearing time is further increased, the system is likely to lose stability in Case-2.

To compare the performance of two modes of operation on transient stability improvement, the fault clearing time is increased by half a cycle and the same contingency is simulated. The response of WTIG speed is shown in Figure 13. The system is unstable without STATCOM and not shown in figure. It can be seen from Figure 13 that, when the STATCOM is operating in voltage control mode (Case-2), the system loses stability due to the tripping of the WTIGs by the protection system. In case of STATCOM operating in var control mode (Case-3), stability of the system is maintained. This is due to the fact that for the same operating condition, the reactive power drawn from the distribution network ( $Q_{DRN}$ ) is more in Case-2 and so the machines are slightly

overloaded compared to Case-3. Hence, the var control mode of operation of STATCOM improves the stability compared to the voltage control mode of operation.

**Linear Change of Wind Speed**

A linear change of wind speed as shown in Figure 8 is applied to the wind turbine. This type of wind speed change enables the wind turbine to inject active power into a network from minimum to maximum value in a manner slow enough not to induce unwanted oscillations. The active power injected to the distribution network ( $P_{INJ}$ ) and reactive power drawn from the distribution network ( $Q_{DRN}$ ) are shown in Figure 14 for the case of without STATCOM. It is clear from Figure 14 that, as the maximum wind speed reaches 11 m/s, the active power injected to the network increases to 9.0 MW compared to constant wind speed (9 m/s) generation of 8.71 MW. It is also evident from Figure 14 that, the reactive power requirement of WTIG increases with the increase in the active power generation and at the maximum  $P_{INJ}$ ,  $Q_{DRN}$  reaches a value of 4.68 MVAR.

A 3-phase fault is applied at the bus 5, at  $t=10$  s and cleared after 5-cycles. The original system is restored upon the fault clearance. The responses of WTIG terminal voltage, the active power injected into the network, the reactive power drawn from the network by the WTIG and WTIG speed are shown in Figures 15 to 18, respectively. It is clear from these figures that, for the system without STATCOM, the WTIG terminal voltage drops to a low value because of the lack of sufficient reactive power support. This low voltage condition results in tripping of WTIGs by the AC Under voltage protection.

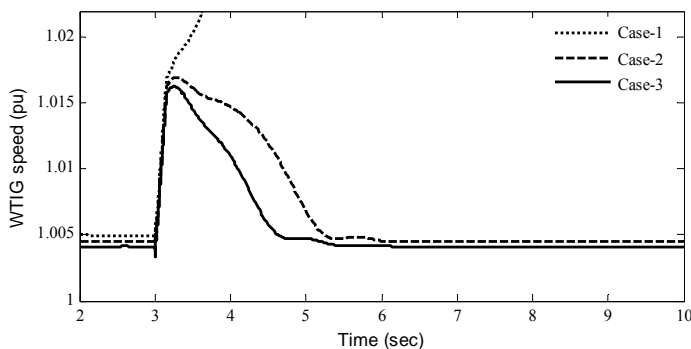


Fig. 12. Response of WTIG speed for 9-cycle, 3-phase fault at bus 5 with constant wind speed.

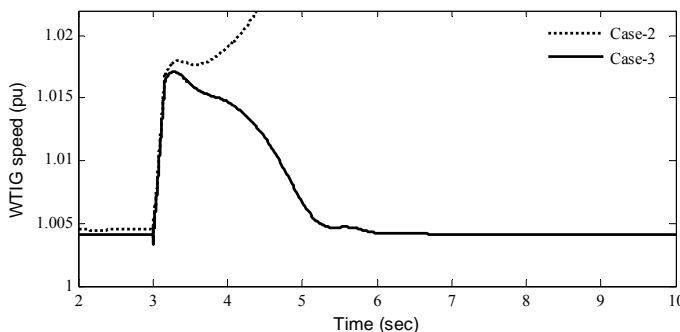


Fig. 13. Response of WTIG speed for 9 and 1/2 cycle, 3-phase fault at bus 5 with constant wind speed.



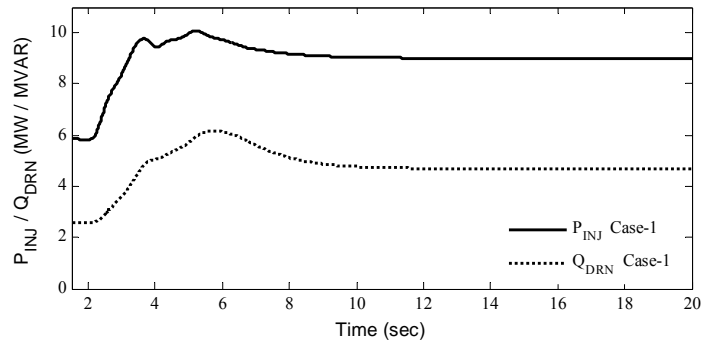


Fig. 14. Active power injected and reactive power drawn with linear change of wind speed.

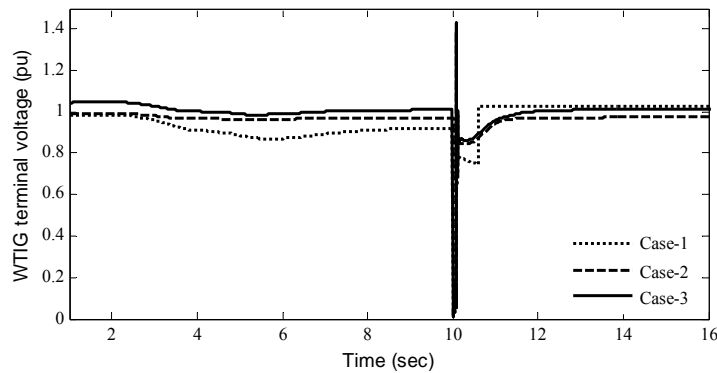


Fig. 15. WTIG terminal voltage response for 5-cycle, 3-phase fault at bus 5 with linear change of wind speed.

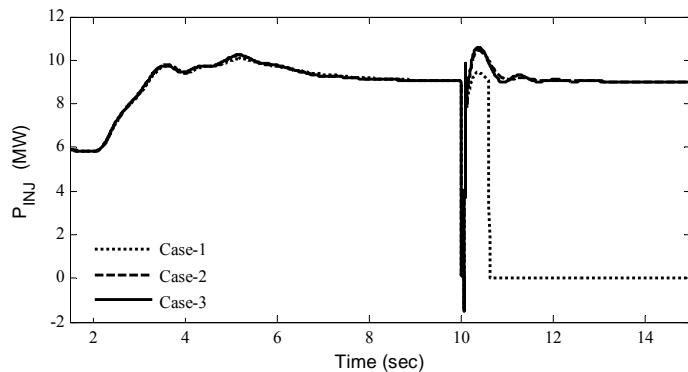


Fig. 16. Response of active power injected for 5-cycle, 3-phase fault at bus 5 with linear change of wind speed.

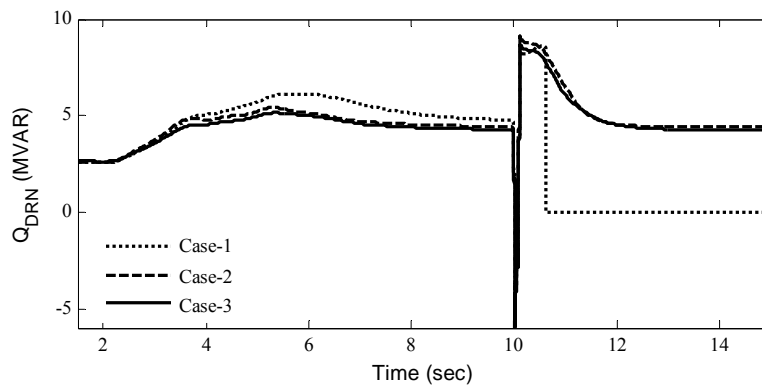


Fig. 17. Response of reactive power drawn from the distribution network for 5-cycle, 3-phase fault at bus 5 with linear change of wind speed.

To compare the performance of two modes of operation in improving the stability, a 3-phase fault of 5 and half cycle duration is applied at the bus 5, at  $t=10$  s. The original system is restored upon the fault clearance. The response of the WTIG speed is shown in Figure 19. The system is unstable without STATCOM (not shown in figure). The WTIG speed response for the cases of system with STATCOM, operating in voltage control mode and

var control modes are shown with legends Case-2 and Case-3 respectively. After the initial transients, the pre-fault WTIG speed settles to around 1.005 pu and 1.004 pu for voltage control and var control mode, respectively. On the occurrence of the fault at  $t=10$  s, the WTIG speed increases suddenly for both cases.

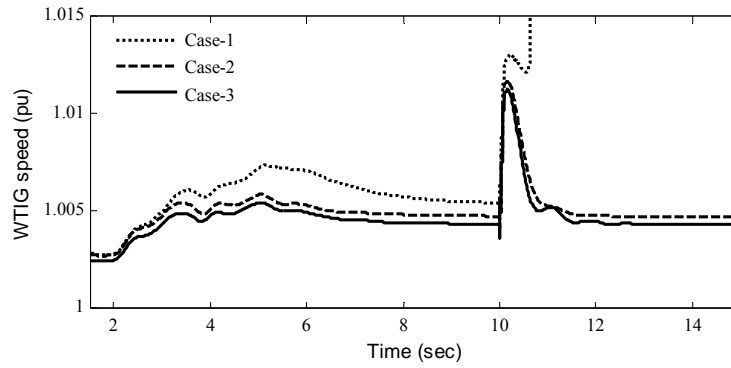


Fig. 18. Response of WTIG speed for 5-cycle, 3-phase fault at bus 5 with linear change of wind speed.

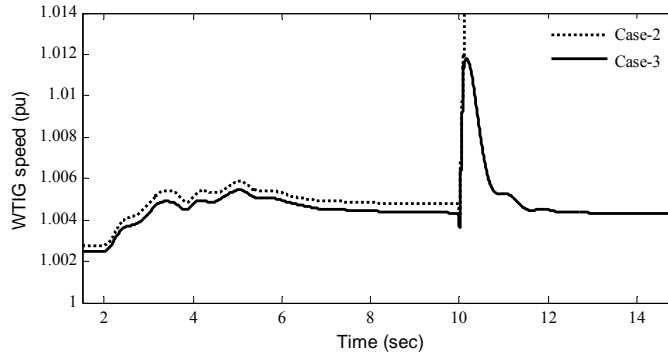


Fig. 19. Response of WTIG speed for 5 and 1/2 cycle, 3-phase fault at bus 5 with linear change of wind speed.

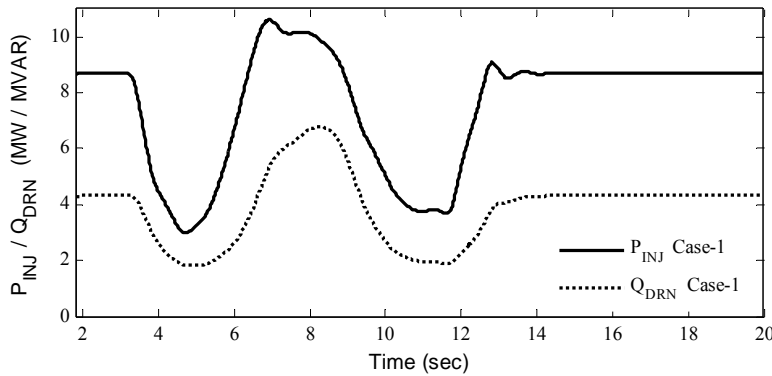


Fig. 20. Active power injected and reactive power drawn with gust change of wind speed.

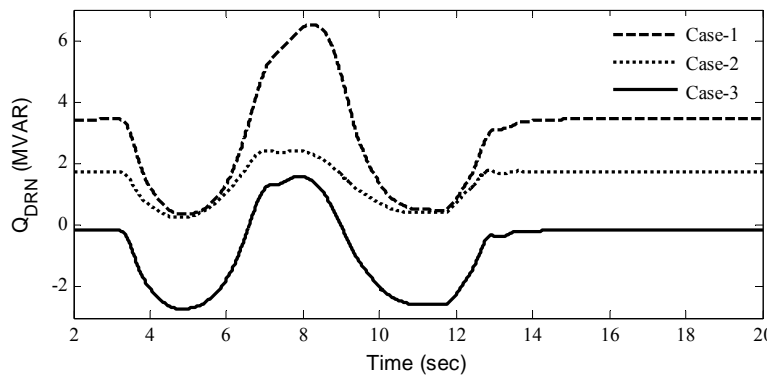


Fig. 21. Response of reactive power drawn from the distribution without and with STATCOM network with gust change of wind speed.

It can be seen from Figure 19 that in Case-2, the system stability is lost due to the tripping of the WTIGs by the protection system. For Case-2, the WTIGs are slightly more overloaded than that for Case-3 to draw more reactive power from the distribution network. On the occurrence of the fault, the WTIG terminal voltage drops to a lower value in Case-2 compared to Case-3. This low voltage condition results in tripping of the WTIGs in

Case-2. However, in Case-3, the stability of the system is maintained as the pre-fault WTIG terminal voltage was comparatively higher for Case-3 and upon the occurrence of the fault, the WTIG terminal voltage drops to a value which is within the limit set by the protection system. Hence, stability of the system is maintained in the Case-3.

### Gust Change of Wind Speed

Gust change of the wind speed is applied here to illustrate the capability of the STATCOM to simultaneously maintain voltage profile and minimize the reactive power exchange between the WTIGs and the distribution network. The gust change is defined as periods of 9.42 s with 22.22 % maximum deviation from the initial value of the wind speed of 9 m/s as shown in Figure 8. The active power injected to the distribution network ( $P_{INJ}$ ) and reactive power drawn from the distribution network ( $Q_{DRN}$ ) are shown in Figure 20 for the case of without STATCOM (Case-1). It is evident from Figure 20 that, with gust change in wind speed, the  $P_{INJ}$  and  $Q_{DRN}$  varies in the same manner (i.e. decreases with decrease in wind speed and vice versa) as shown in Figure 20.

The variation of  $Q_{DRN}$  for gust change of wind speed is shown in Figure 21, for all the cases. For the system without STATCOM (Case-1),  $Q_{DRN}$  in the pre-disturbance and post-disturbance period is highest compared to the other cases and equals to 3.45 MVAR. The corresponding values for voltage control mode and var control mode of operation of STATCOM (Case-2 and Case-3) are 1.75 and -0.15 MVAR respectively. The negative value of  $Q_{DRN}$  indicates that, reactive power is supplied to the grid. Further, it can be observed from Figure 21 that, for Case-1, the value of  $Q_{DRN}$  increases to 6.52 MVAR at the maximum wind speed of 11 m/s at  $t=8$  s, whereas the corresponding values for Case-2 and Case-3 are 2.43 and 1.59 MVAR respectively. The difference in  $Q_{DRN}$  for Case-2 and Case-3 is due to the fact that, in Case-3 the STATCOM supplies more reactive power.

### Linear Change of Wind Speed

To illustrate the capability of the STATCOM to maintain voltage profile and minimize the reactive power exchange between the WTIGs and the distribution network, random change of wind speed shown in Figure 8, is considered. With random change in wind speed,  $Q_{DRN}$  also varies in the same random manner. Figure 22 shows the variation of  $Q_{DRN}$  for random change of wind speed for all the cases. It is clear from the Figure 22 that, for the system without STATCOM (Case-1), the variation in  $Q_{DRN}$  is maximum (4.294 MVAR) because of the absence of dynamic reactive power compensation. For Case-2, the controller tries to maintain the terminal voltage constant and so the distribution system draws that much reactive power; the maximum value of  $Q_{DRN}$  being equal to 2.07 MVAR. But in Case-3, the STATCOM tries to supply the rated

reactive power.  $Q_{STATCOM}$  in Case-3 is sometimes more than the reactive power requirement of the WTIGs and hence  $Q_{DRN}$  is negative in that case. Negative  $Q_{DRN}$  implies that reactive power is supplied to the distribution network. In Case-3,  $Q_{DRN}$  varies from -2.73 to 0.448 MVAR.

### Impact of Wind Speed on Terminal Voltage

In order to investigate the effect of different types of wind speed changes on the variation of bus voltage magnitudes, all four types of wind speed are considered. Figures 23 to 26 show the variation of WTIG terminal voltage for all four types of wind speeds and for all the three cases.

In these figures the legends A, B, C, D indicate constant, linear change, gust change and random change in wind speed respectively and the subscript 1, 2 and 3 indicate the three cases (Cases-1, 2 and 3). For constant wind speed of 9 m/s, as shown in Figure 23, the WTIG terminal voltage for the case of system without STATCOM ( $A_1$ ) is 0.9486 pu and the corresponding values with STATCOM operating in voltage control mode ( $A_2$ ) and var control mode ( $A_3$ ) are 0.9861 pu 1.0125 pu, respectively.

With linear increase in wind speed, the real power output of WTIGs increases and hence the reactive power consumption also increases. Figure 24 shows the WTIG terminal voltage variation for linear change of wind speed from 8 to 11 m/s, for all the cases. The terminal voltages at the minimum wind speed of 8 m/s are 0.9892 pu, 0.9966 pu and 1.0149 pu for Case-1, 2 and 3 respectively. During the transient period the same drops to 0.8938 pu, 0.9768 pu and 0.9995 pu for Cases-1, 2 and 3 respectively. WTIG terminal voltage finally settles at 0.9395 pu, 0.9844 pu and 1.02 pu respectively for Case-1 ( $B_1$ ), Case-2 ( $B_2$ ) and Case-3 ( $B_3$ ) respectively. WTIG terminal voltage variation for gust change of wind speed is shown in Figure 25. It can be seen from Figure 25 that, the WTIG terminal voltages in the pre-disturbance and post-disturbance period are 0.9486 pu, 0.9861 pu and 1.025 pu for Case-1 ( $C_1$ ), Case-2 ( $C_2$ ) and Case-3 ( $C_3$ ) respectively. At the maximum wind speed of 11 m/s at  $t=8$  s, the terminal voltage drops to 0.871 pu, 0.974 pu and 0.9917 pu for Case-1, Case-2 and Case-3 respectively. The terminal voltage reaches a maximum value of 0.9996 pu, 0.9996 pu and 1.055 pu for Case-1, Case-2 and Case-3 respectively at minimum wind speed of 7 m/s.

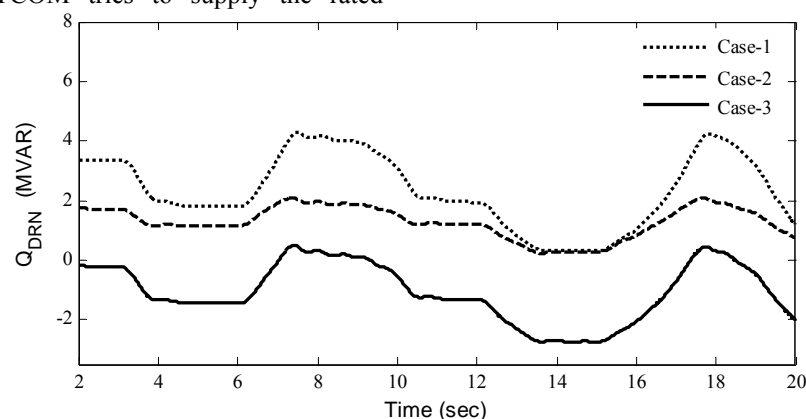


Fig. 22. Response of reactive power drawn from the distribution network without and with STATCOM with random change of wind speed

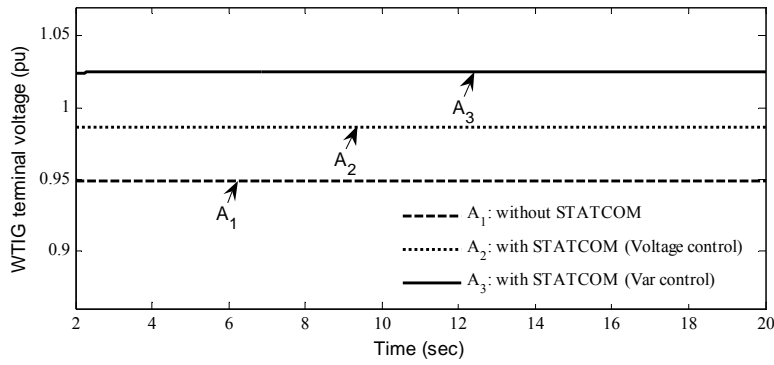


Fig. 23. WTIG terminal voltage response with constant wind speed of 9 m/s.

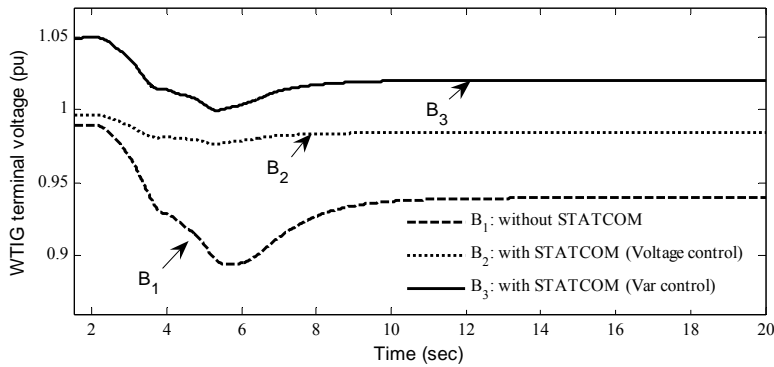


Fig. 24. WTIG terminal voltage response with linear change of wind speed from 8 to 11 m/s.

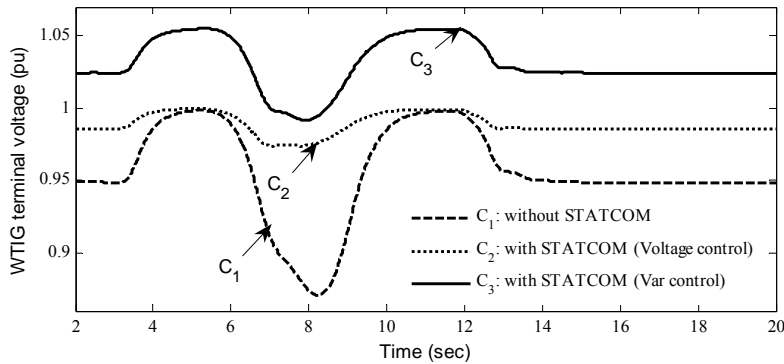


Fig. 25. WTIG terminal voltage response with gust change of wind speed.

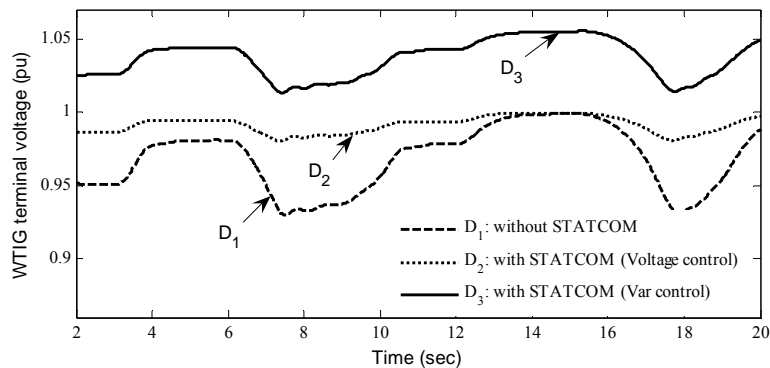


Fig. 26. WTIG terminal voltage response with random change of wind speed

Figure 26 shows the WTIG terminal voltage variation for random change of wind speed. It can be seen from Figure 26 that, for the system without STATCOM (D<sub>1</sub>) the WTIG terminal voltage varies from a minimum value of 0.9298 pu (at maximum wind speed of 9.64 m/s) to 0.9989 pu (at minimum wind speed of 7.19 m/s). The corresponding values are 0.9805 pu and 0.9996 pu for

Case-2 (D<sub>2</sub>) and 1.013 pu and 1.055 pu for Case-3 (D<sub>3</sub>).

It is clear from the Figures 23-26 that, for the cases of system without STATCOM (A<sub>1</sub>, B<sub>1</sub>, C<sub>1</sub> and D<sub>1</sub>), because of absence of dynamic reactive power compensation, WTIG terminal voltage decreases and its variation is maximum. For the cases of STATCOM in voltage control mode i.e. Case-2 (A<sub>2</sub>, B<sub>2</sub>, C<sub>2</sub> and D<sub>2</sub>),

voltage variation is minimum. Also, in Case-2, the voltage magnitudes are nearer to 1 pu for all types of wind speed, as the controller tries to maintain the voltage constant. The variation of WTIG terminal voltage is more in Case-3 ( $A_3$ ,  $B_3$ ,  $C_3$  and  $D_3$ ), compared to the Case-2. Further, the voltage magnitude is more than 1 pu for Case-3, as the STATCOM supplies the rated reactive power.

## 6. CONCLUSION

A comprehensive study about the stability performance improvement of a distribution network embedded with Wind Turbine Induction Generators (WTIG) using a Static Synchronous Compensator (STATCOM) has been presented. Different types of wind speeds and different control modes of operation of STATCOM are considered in the present analysis. Simulation results show that the FACTS based reactive power compensation prevents large deviations of bus voltage magnitude induced by reactive power drawn from distribution network by WTIGs and helps to maintain the system stability. It is observed that, after being subjected to an external fault, the var control mode is more effective in maintaining the system stability so that the WTIGs remain connected to the distribution system running at a speed corresponding to the system frequency. This is due to the fact that, the reactive power supplied in var control mode of operation of STATCOM is more than that of voltage control mode and hence the pre-fault WTIG terminal voltage is more in var control mode. For all types of wind speed changes, the variation in WTIG terminal voltage magnitude is less when the STATCOM is operated under voltage control mode compared to the var control mode.

## REFERENCES

- [1] OECD/IEA. Wind Power Integration into Electricity Systems, Case Study 5. [Online serial], Retrieved July 23, 2007 from the World Wide Web: <http://www.oecd.org/env/cc/>
- [2] Jenkins, N., Allan, R., Crossley, P., Kirschen, D. and Strabac, G., 2000. *Embedded Generation*. United Kingdom: IEE Power and Energy Series.
- [3] Jurado, F. and Carpio, J., 2005. Enhancing the distribution networks stability using distributed generation. *The International Journal for Computation and Mathematics in Electrical and Electronic Engineering* 24: 107-26.
- [4] Vittal, V., 2000. Consequence and impact of electric utility industry restructuring on transient stability and small-signal stability analysis. *IEEE Proceedings* 88: 196-207.
- [5] Hatziaargyriou, N.D. and Meliopoulos, A.P.S., 2002. Distributed energy sources: technical challenges. *Proceedings of IEEE Power Engineering Society Winter Meeting* 2:1017-1022.
- [6] Gnativ, R. and Milanovi, J.V., 2001. Voltage sag propagation in systems with embedded generation and induction motors. *IEEE Power Engineering Society Summer Meeting* 1:474 – 479.
- [7] Freitas, W., Asada, E., Morelato, A. and Wilsun, X., 2002. Dynamic improvement of induction generators connected to distribution systems using a DSTATCOM. In *Proceedings of the International Conference on Power System Technology*.

*POWERCON 2002*, Kunming, China. 13-17 October, New York: IEEE Press.

- [8] Hingorani, N.G. and Gyugyi, L., 2000. *Understanding FACTS: Concepts and Technology of Flexible AC Transmission Systems*. New York: IEEE Press..
- [9] Gyugyi, L., 1994. Dynamic compensation of ac transmission lines by solid-state synchronous voltage sources. *IEEE Transactions on Power Delivery* 9: 904-911.
- [10] Arulampalam, A., Barnes, M., Jenkins, N. and Ekanayake, J.B., 2006. Power quality and stability improvement of a wind farm using STATCOM supported with hybrid battery energy storage. *IEE Proceedings Generation, Transmission and Distribution*, 153(6): 701-710.
- [11] Chen, Z., Blaabjerg, F. and Hu, Y., 2006. Stability improvement of wind turbine systems by STATCOM. In *Proceedings of the Thirty Second Annual IEEE Industrial Electronics International conference, IECON 2006*, Paris, France, 7-10 November, New York: IEEE Press.
- [12] Gaztanaga, H., Etcheberria-Otadui, I., Ocnasu, D., and Bacha, S., 2007. Real-time analysis of the transient response improvement of fixed-speed wind farms by using a reduced-scale STATCOM Prototype. *IEEE Transactions on Power Systems* 22(2): 658-666.
- [13] SimPowerSystems 4.3 User's Guide, Available: <http://www.mathworks.com/products/simpower/>
- [14] Samuelsson, O. and Lindahl, S., 2005. On speed stability. *IEEE Transactions on Power Systems* 20 (2): 1179 – 1180.

## APPENDIX

System data: All data are in pu unless specified otherwise.

### Transformer: Substation transformer

Nominal power:  $S_B = 47$  MVA

Winding connections:  $Y_g/D_1$  connection

Winding parameters:  $V_1 = 120$  kV,  $V_2 = 25$  kV

$$R_1 = R_2 = 0.0027$$

$$L_1 = 0, L_2 = 0.08$$

Magnetization resistances:  $R_m = 500$

Magnetization reactances:  $L_m = 500$

### WTIG to distribution network transformers

Nominal powers:  $S_B = 4$  MVA

Winding connections:  $Y_g/Y_n$  connection

Winding parameters:  $V_1 = 25$  kV,  $V_2 = 575$  V

$$R_1 = R_2 = 0.833 \times 10^{-3}$$

$$L_1 = 0, L_2 = 0.025$$

Magnetization resistances:  $R_m = 500$

Magnetization reactances:  $L_m = \text{Inf}$ .

### Transmission line:

Positive and zero sequence resistances:

$$R_1 = 0.1153 \Omega/\text{km}, R_0 = 0.413 \Omega/\text{km}$$

Positive and zero sequence inductances:

$$L_1 = 1.05 \text{ mH/km}, L_0 = 3.32 \text{ mH/km}$$

Positive and zero sequence capacitances:

$$C_1 = 11.33 \times 10^{-9} \text{ F/km}, C_0 = 5.01 \times 10^{-9} \text{ F/km}$$

#### Line lengths

Bus 2-3 and 3-4 = 10 km

Bus 4-5 = 5 km

Bus 5-6, 5-7 and 5-8 = 1 km.

#### Loads (kW + j kVAR)

Load 1 = 5000+j1000

Loads 2, 3 and 4 = 500+j20

Load 5 = 1000+j50

#### Wind Turbine Induction generator (WTIG):

##### Turbine

Nominal wind turbine mechanical output power:

$$P_B = 3 \text{ MW}$$

Base wind speed:  $v_{wind} = 9 \text{ m/s}$

Pitch angle controller gain:  $K_p = 5, K_i = 25$

Maximum pitch angle:  $\beta_{max} = 45^\circ$

Maximum rate of change of pitch angle =  $2^\circ \text{ deg/s}$

Coefficients:  $c_1 = 0.5176, c_2 = 116, c_3 = 0.4$

$$c_4 = 5, c_5 = 21 \text{ and } c_6 = 0.0068$$

#### Generators

Nominal power:  $S_B = 3.33 \text{ MVA}$

Nominal voltage:  $V_B = 575 \text{ V}$

Nominal frequency:  $f = 60 \text{ Hz}$

Stator resistance and reactance:  $R_s = 0.004843,$

$$L_{ls} = 0.1248$$

Rotor resistance and reactance:  $R'_r = 0.004377,$

$$L'_{lr} = 0.1791$$

Magnetizing inductance:  $L_m = 6.7$

Inertia constant, friction factor and pair of poles:

$$H = 5.04, F = 0.01, p = 3$$

#### STATCOM:

Converter rating:  $S_{nom} = 3 \text{ MVA}$

System nominal voltage:  $V_{nom} = 25 \text{ kV}$

Frequency:  $f = 60 \text{ Hz}$

Converter impedance:  $R = 0.073, L = 0.22$

DC link nominal voltage:  $V_{DC} = 4 \text{ kV}$

DC link equivalent capacitance:  $C_{DC} = 0.0011 \text{ F}$

Droop = 0.03

AC voltage regulator gains:  $K_p = 5, K_i = 1000$

DC voltage regulator gains:  $K_p = 1 \times 10^{-3}$

$$K_i = 20 \times 10^{-3}$$

Current regulator gains:  $K_p = 0.3, K_i = 10$

$$K_f = 0.22$$